

A PERFORMANCE CHARACTERISATION IN ADVANCED DATA SMOOTHING TECHNIQUES

Michael Lynch*, Kevin Robinson, Ovidiu Ghita, Paul F. Whelan
Vision Systems Group
Dublin City University, Ireland

Abstract

A comparison paper is presented to evaluate the results from five smoothing filters. The filters are linear, nonlinear isotropic and nonlinear anisotropic designed to smooth homogenous areas while preserving the higher moments in the data. The methods are outlined and then evaluated on the extent to which edge information is preserved and unwanted noise is suppressed.

Keywords: *Smoothing, adaptive, Savitzky-Golay, diffusion*

1 Introduction

The process of smoothing images is two-fold, firstly to remove unwanted noise from the image to facilitate further processing and secondly to maintain important image features such as edges.

There are two main types of smoothing, linear and non-linear. Both of these types have been extensively studied in literature. One of the main aims of filtering images is to smooth areas of homogeneity and to preserve areas of interest such as edges. Traditional linear filters such as mean, average and Gaussian attempt to remove noise by replacing each pixel by an average or weighted average of its spatial neighbours [2]. While this reduces the amount of noise present in the image, it also has the disadvantage of removing or blurring the edges. Nonlinear filters, the most common being the median filter, modifies the value of the pixel by some nonlinear function of the pixel value and its spatial neighbours. Nonlinear filters maintain the edges but the filtering results in a loss of resolution by suppressing fine details. More recently, the use of edge-based diffusion has emerged [1, 3, 4, 5, 6]. These filters require a tradeoff between smoothing efficiency, preservation of discontinuities and the generation of artifacts. In short the diffusion or smoothing term is a variable over space and time and in [3], this term is a function of the magnitude of the gradient intensity at the point in question. Gerig [4] extended this case to 3D and performed the diffusion on medical volumes. Perona and Malik's [3] diffusion has the disadvantage that it stopped the diffusion at edges, this was advanced by [7] by permitting diffusion along the direction of the edges making it anisotropic.

This paper compares five filters. The linear Savitzky-Golay filter is a convolution of the image with the least-squares fitting of a polynomial. The basic linear Gaussian filter is a convolution with a gaussian mask, nonlinear adaptive filtering which filters the image but smooths less in areas of local discontinuities and high spatial variance. Nonlinear diffusion, which again smooths with an exponential with no smoothing occurring where the gradient has high values. Finally anisotropic gaussian smoothing which uses a scaled and shaped gaussian mask to smooth along the direction of high gradients and never across the gradients.

*Corresponding author. *E-mail address:* lynchm@eeng.dcu.ie

2 Savitzky-Golay Filter

The Savitzky-Golay [8] smoothing filter was introduced for smoothing data and for computing the numerical derivatives. The smoothed points are found by replacing each data point with the value of its fitted polynomial. The process of Savitzky-Golay is to find the coefficients of the polynomial which are linear with respect to the data values. Therefore the problem is reduced to finding the coefficients for fictitious data and applying this linear filter over the complete data. The size of the smoothing window is given as $N \times N$ where N is odd, and the order of the polynomial to fit is k , where $N > k + 1$. The general smoothing causal filter equation is given as;

$$g_{x,y} = \sum_{j=-n}^n \sum_{i=-n}^n C_{i,j} f_{x+i,y+j} \quad (1)$$

n is equal to $\frac{N-1}{2}$. C is the convolution matrix and f_{xy} is the original data.

$$f(x_i, y_i) = a_{00} + a_{10}x_i + a_{01}y_i + a_{20}x_i^2 + a_{11}x_iy_i + a_{02}y_i^2 + \dots + a_{0k}y_i^k \quad (2)$$

We then want to fit a polynomial of type in equation (2) to the data. Solving the least squares we can find the polynomial coefficients. We start of the the general equation;

$$A \cdot a = f$$

where a is the vector of polynomial coefficients

$$a = (a_{00} \quad a_{01} \quad a_{10} \quad \dots \quad a_{0k})^T$$

We can then compute the coefficient matrix as follows.

$$(A^T \cdot A) \cdot a = (A^T \cdot f)$$

$$a = (A^T \cdot A)^{-1} \cdot (A^T \cdot f)$$

Due to the linear-squares fitting being linear to the values of the data, the coefficients can be computed independent of data. To achieve this we can replace f with a unit vector thus, the coefficient matrix becomes $C = (A^T A)^{-1} A^T$. C can then be reassembled back into a traditional looking filter of size $N \times N$. In order to smooth the image the first coefficient is used, higher order coefficients are used to calculate derivatives. The advantage of the Savitzky-Golay filter has over moving average and other FIR filters is its ability to preserve higher moments in the data and thus reduce smoothing on peak heights. In more homogenous areas the smoothing approaches an average filter over the smoothing kernel.

3 Adaptive Smoothing

The algorithm for adaptive smoothing implemented in this paper is adapted from Chen [5]. The technique measures two types of discontinuities in the image, local and spatial. From both these measures a less ambiguous smoothing solution is found. In short, the local discontinuities indicate the detailed local structures while the contextual discontinuities show the important features.

In order to measure the local discontinuities, four detectors are set up as shown:

$$E_{H_{xy}} = |I_{x+1,y} - I_{x-1,y}|, \quad (6)$$

$$E_{V_{xy}} = |I_{x,y+1} - I_{x,y-1}|, \quad (7)$$

$$E_{D_{xy}} = |I_{x+1,y+1} - I_{x-1,y-1}|, \quad (8)$$

$$E_{C_{xy}} = |I_{x+1,y-1} - I_{x-1,y+1}|, \quad (9)$$

$I_{x,y}$ is the intensity of the pixel at the position (x,y). We can then define a local discontinuity measure E_{xy} as:

$$E_{xy} = \frac{E_{H_{xy}} + E_{V_{xy}} + E_{D_{xy}} + E_{C_{xy}}}{4} \quad (10)$$

In order to measure the contextual discontinuities, a spatial variance is employed. First, a square kernel is set up around the pixel of interest, $N_{xy}(R)$. The mean intensity value of all the members of this kernel is calculated for each pixel as follows:

$$\mu_{xy}(R) = \frac{\sum_{(i,j) \in N_{xy}(R)} I_{i,j}}{|N_{xy}(R)|} \quad (11)$$

From the mean the spatial variance is then calculated to be:

$$\sigma_{xy}^2(R) = \frac{\sum_{(i,j) \in N_{xy}(R)} (I_{i,j} - \mu_{xy}(R))^2}{|N_{xy}(R)|} \quad (12)$$

This value of sigma is then normalised to $\tilde{\sigma}_{xy}^2$ between the minimum and maximum variance in the entire image. A transformation is then added into $\tilde{\sigma}_{xy}^2$ to alleviate the influence of noise and trivial features. It is given a threshold value of $\theta_\sigma = (0 \leq \theta_\sigma \leq 1)$ to limit the degree of contextual discontinuities.

Finally, the actual smoothing algorithm runs through the entire image updating each pixels intensity value I_{xy}^t , where t is the iteration value.

$$I_{xy}^{t+1} = I_{xy}^t + \eta_{xy} \frac{\sum_{(i,j) \in N_{xy}(1)/\{(x,y)\}} \eta_{ij} \gamma_{ij}^t (I_{i,j}^t - I_{x,y}^t)}{\sum_{(i,j) \in N_{xy}(1)/\{(x,y)\}} \eta_{ij} \gamma_{ij}^t} \quad (13)$$

where,

$$\eta_{ij} = \exp(-\alpha \Phi(\tilde{\sigma}_{xy}^2(R), \theta_\sigma)), \quad (14)$$

$$\gamma_{ij}^t = \exp(-E_{ij}^t/S) \quad (15)$$

The variables S and α determine to what extent the local and contextual discontinuities should be preserved during smoothing. If there are a lot of contextual discontinuities in the image then the value of η_{ij} will have a large influence on the updated intensity value. On the other hand, if there are a lot of local discontinuities then both γ_{ij} and η_{ij} will have the overriding effect, as η_{ij} is used for gain control of the adaption.

4 Nonlinear Diffusion Filtering

The standard blurring operation involving Gaussian filtering attempts to remove the noise at the expense of poor edge preservation. The Gaussian smoothing technique is very straightforward and involves the convolution of the original image with a 2D Gaussian where the standard deviation selects the scale of the blurring operation.

$$S_{x,y} = I_{x,y} \circ \text{Gauss}(x, y, \sigma) \quad (16)$$

$$\text{Gauss}(x, y, \sigma) = \frac{1}{2\pi\sigma^2} e^{-\frac{x^2+y^2}{2\sigma^2}} \quad (17)$$

where S is the filtered image, I is the input image, \circ implements the 2D convolution, $\text{Gauss}()$ is the 2D Gaussian function where σ is the scale parameter. From Eq. 17 becomes obvious that the smoothing

becomes more pronounced for higher values of the scale parameter but at the same time we can notice a significant attenuation of the optical signal associated with image boundaries. This result is highly undesirable for many applications including image segmentation and edge tracking where a precise identification of the object boundary is required.

To alleviate the problems associated with the standard Gaussian smoothing technique, Perona and Malik [3] proposed an elegant smoothing scheme based on non-linear diffusion. In their formulation the blurring would be performed within homogenous image regions with no interaction between adjacent or neighbouring regions that share a common border. The non-linear diffusion procedure can be written in terms of the derivative of the flux function:

$$\phi(\nabla I) = \nabla I \cdot D(\|\nabla I\|) \quad (18)$$

where ϕ is the flux function, I is the image and D is the diffusion function. Eq. 18 can be implemented in an iterative manner and the expression required to implement the non-linear diffusion is illustrated in Eq. 19.

$$I_{x,y}^{t+1} = I_{x,y}^t + \lambda \sum_{R=1}^4 [D(\nabla_R I) \nabla_R I]^t \quad (19)$$

where I^t represents the image at iteration t , R defines the 4-connected neighbourhood, D is the diffusion function, ∇ is the gradient operator that has been implemented as the 4 connected nearest-neighbour differences and λ is a parameter that takes a values in the range $0 < \lambda < 0.25$.

$$\begin{aligned} \nabla_1 I_{x,y} &= I_{x-1,y} - I_{x,y} \\ \nabla_2 I_{x,y} &= I_{x+1,y} - I_{x,y} \\ \nabla_3 I_{x,y} &= I_{x,y-1} - I_{x,y} \\ \nabla_4 I_{x,y} &= I_{x,y+1} - I_{x,y} \end{aligned} \quad (20)$$

The diffusion function $D(x)$ should be bounded between 0 and 1 and should have the peak value when the input x is set to zero. This would translate with no smoothing around the region boundary where the gradient has high values. In practice, a large number of functions can be implemented to satisfy this requirement and in our implementation we were using the exponential function proposed by Perona and Malik [3].

$$D(\|\nabla I\|) = e^{-\left(\frac{\|\nabla I\|}{k}\right)^2} \quad (21)$$

where k is the diffusion parameter. The parameter k selects the smoothness level and the smoothing effect is more noticeable for high values of k .

5 Anisotropic Gaussian Smoothing

An anisotropic filter based on the familiar gaussian model was implemented in order to provide edge enhancing, directional smoothing. The goal was to develop a versatile smoothing filter based on a straightforward and highly adaptable form. The approach reduces to convolution with a scaled and shaped gaussian mask, where the determination of the mask weights becomes the key step governing the performance of the filter. By calculating the local greyscale gradient vector and favouring smoothing along the edge over smoothing across it we can achieve an effective boundary preserving filtering approach, where regions are homogenised while edges are retained.

The weight $wt(p\vec{q}, \nabla u)$ at each location in the mask is a function of the local gradient vector at the centre of the mask and the distance of the current neighbour from that centre. There is a large number

	<i>Laboratory Image</i>	<i>MR Image</i>
Original	57.4	277.65
Savitzky-Golay	40.804	61.232
Gaussian	40.966	102.08
Adaptive	24.241	42.99
Diffusion	27.658	69.633
Anisotropic	31.905	35.05

Table 1: The RMS of the standard deviation of the homogenous areas for the original and each filtered image

of possibilities for the formulation of the mask weight calculation, based on the desired form for the non-linear and anisotropic components of the filter. The weight for some neighbour q is calculated as a function of the gradient of point p , at the mask origin, and the distance from the origin to the neighbour q . The relationship used in our approach is given in Eq. 22, where \vec{pq} is the vector from the mask centre point p to some neighbour q , ∇u is the gradient vector at p , λ is the scale parameter, controlling smoothing strength, and μ is the shape parameter, controlling anisotropy. When μ equals zero the anisotropic term $(\frac{\vec{pq} \cdot \nabla u}{\lambda})^2 (2\mu + \mu^2)$ disappears and the filter reduces to the non-linear, isotropic form, where smoothing decreases close to strong edges but is applied equally in all directions, at any given location in the image.

$$wt(\vec{pq}, \nabla u) = e^{-((\frac{\|\vec{pq}\| \|\nabla u\|}{\lambda})^2 + (\frac{\vec{pq} \cdot \nabla u}{\lambda})^2 (2\mu + \mu^2))} \quad (22)$$

The images in Figures 1 and 2 illustrate the operation of the anisotropic filter. As the smoothing strength and the number of iterations is increased more noise and small features are eliminated, but even in extreme cases the most important edges in the image are well preserved in both location and strength.

6 Experiments and Results

The aim of each filter evaluated in this study is to smooth areas of homogeneity while preserving areas of interest such as edges. Smoothing of homogenous areas is measured using the standard deviation while the preservation of edges is measured using the strength and spread of the edge in the filtered images. The filters are tested on two images, see figures 1 and 2, the first image of a laboratory having a high SNR (signal-noise-ratio) and high CNR (contrast-to-noise-ratio) with a high density of edges. The second medical image has a much lower SNR and CNR. Parameters were chosen to give the optimal results on visual inspection. Visual results are presented in figure 6.

The standard deviation is measured in a 7×7 window over the entire original image. From these values 25% of the highest values were eliminated as belonging to edges in the image and 25% of the lower values as having no significant texture. The standard deviation for each of the filtered images is then taken at the same positions. The results are presented in Table 1. For the laboratory image, Adaptive smoothing gives the best results followed by the two other non-linear filters. Both linear Savitzky-Golay and Gaussian filters have the highest deviation after smoothing. In the medical image there are more significant differences with the anisotropic and adaptive smoothing operators giving the best results while the gaussian performs worst in the low SNR image.

The strength, shift and spread of the edge is evaluated on each of the images. Histogram plots across two edges are shown in figure 3 showing both the image pixels and the gradient across the edge. For the lab image the results are similar for all filters with more significant differences between filters in the medical image. Two measurements are taken from these histograms which indicate edge strength and spread. These results are compiled in Table 2. While Savitzky-Golay and Gaussian filters spread the edge, the other three maintain and even enhance the edge characteristics.

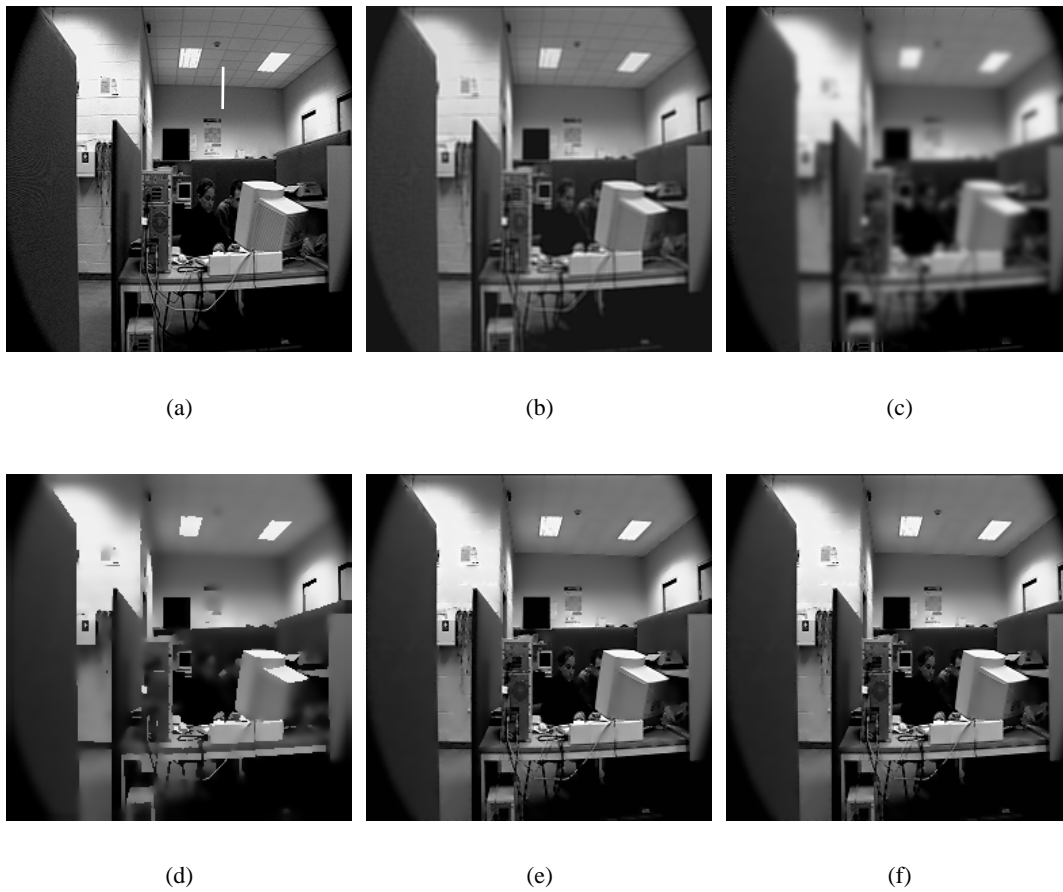


Figure 1: Results from each of the smoothing filters, (a) is the original image, (b) image after Savitzky-Golay, (c) Gaussian, (d) Adaptive, (e) nonlinear diffusion and (f) anisotropic gaussian.

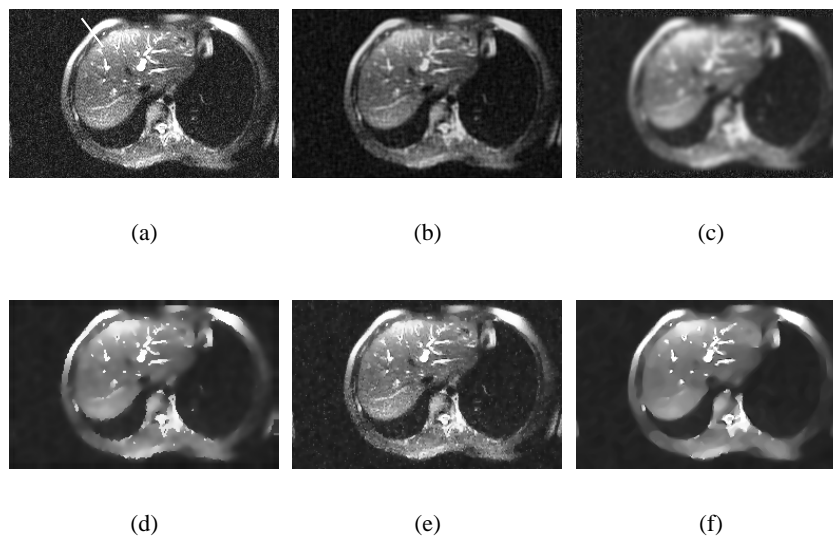


Figure 2: Results from each of the smoothing filters, (a) is the original image, (b) image after Savitzky-Golay, (c) Gaussian, (d) Adaptive, (e) nonlinear diffusion and (f) anisotropic gaussian.

	<i>Laboratory Image</i>		<i>MR Image</i>	
	Edge height	Edge width	Edge height	Edge width
Original	31	2.26	219	2.04
Savitzky-Golay	23	2.5	158	2.48
Gaussian	15	4.4	196	2.16
Adaptive	26	2.13	211	2.00
Diffusion	25	2.17	214	2.00
Anisotropic	30	2.17	219	1.99

Table 2: Shows the edge strength and edge spread on the gradient image after each filtering from histograms in figure 3.

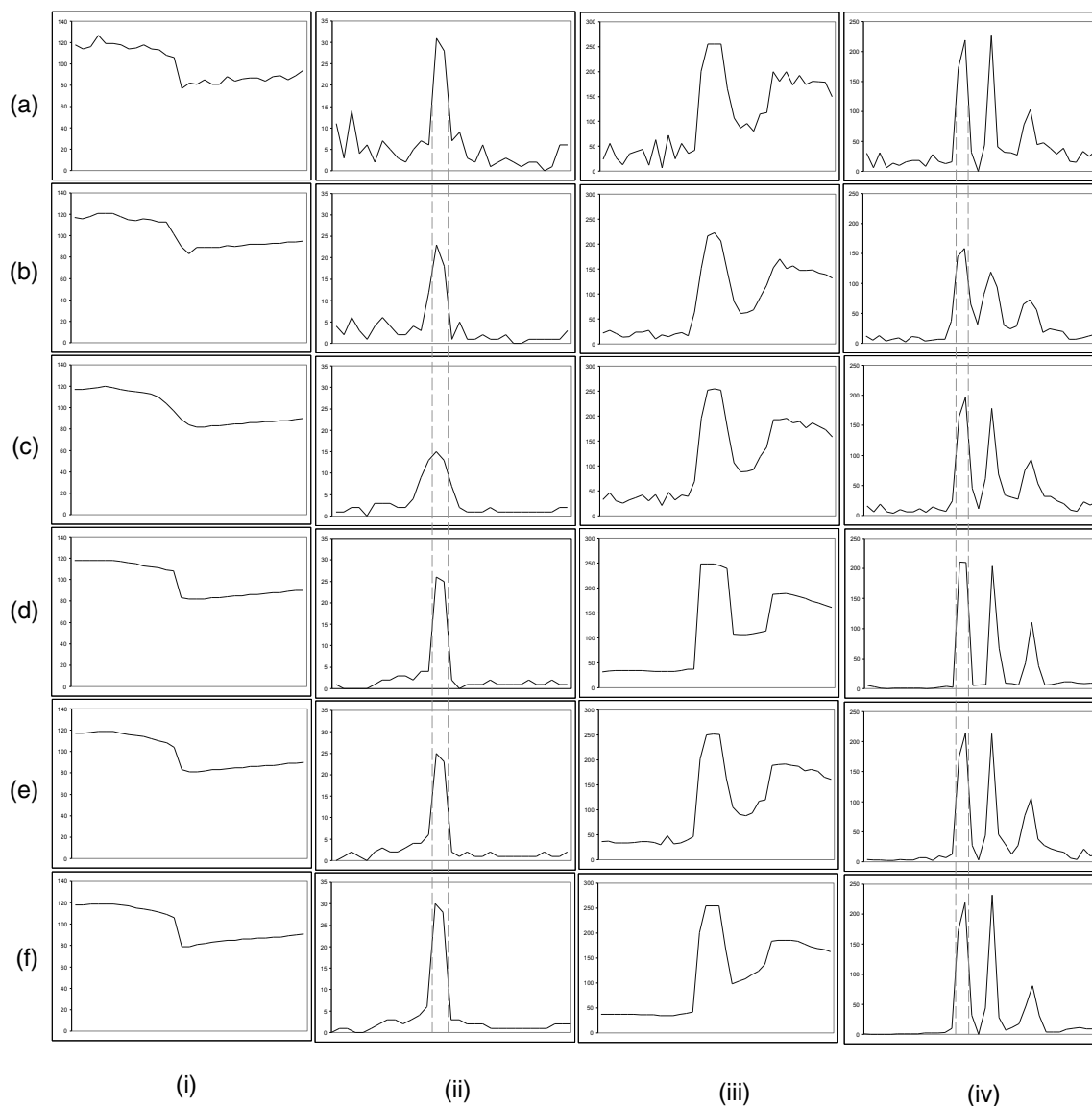


Figure 3: Pixel intensities and gradients along white lines from images *figure 1(a)* and *figure 2(a)*. (i) and (iii) show the pixel intensities and (ii) and (iv) show the gradient values from the lab image and the medical image respectively. (a) is the original image, (b) image after Savitzky-Golay, (c) Gaussian, (d) Adaptive, (e) nonlinear diffusion and (f) anisotropic gaussian.

7 Conclusion

Five filters were evaluated using two criteria, texture smoothing and edge preservation. The filters consisted of two linear filters, two non-linear isotropic and one non-linear anisotropic. The filters were tested on two images with high and low SNR and the results show that, particularly in the low SNR case, the anisotropic and adaptive filters performs much better than the linear filters at smoothing out the noise in homogenous areas while still maintaining the edge strengths with minimum blurring across the edge.

The gaussian performs the worst of all the filters. The Savitzky-Golay deals better at preserving the edges but again suffers in the lower SNR image. The anisotropic and adaptive smoothings preservation of edges allows for more aggressive smoothing on homogenous areas.

References

- [1] J.J Koenderink. The structures of images. *Biological Cybernetics*, 50:363–370, 1984.
- [2] M. Petrou and P. Bosdogianni. *Image Processing: The Fundamentals*. Wiley Publishing, Inc., 1st edition, 1999.
- [3] P. Perona and J. Malik. Scale-space and edge detection using anisotropic diffusion. *IEEE Trans. on Pattern Analysis and Machine Intelligence*, 12(7):629–639, 1990.
- [4] G. Gerig, O. Kbler, R. Kikinis, and F.A. Jolesz. Nonlinear anisotropic filtering of MRI data. *IEEE Transactions on Medical Imaging*, 11(2):221–232, June 1992.
- [5] K. Chen. A Feature Preserving Adaptive Smoothing Method for Early Vision. Technical report, National Laboratory of Machine Perception and The Center for Information Science, Peking University, Beijing, China, 1999.
- [6] G. I. Sanchez-Ortiz, D. Rueckert, and P. Burger. Knowledge-based tensor anisotropic diffusion of cardiac magnetic resonance images. *Medical Image Analysis*, 3(1), 1999.
- [7] J. Weickert. A review of nonlinear diffusion filtering. *Scale-Space Theory in Computer Vision*, 1252:3–28, 1997. Springer, Berlin. B. ter Haar Romeny, L. Florack, J. Koenderink and M. Viergever (Eds.).
- [8] A. Savitzky and M.J.E Golay. Smoothing and differentiation of data by simplified least squares procedures. *Analytical Chemistry*, 36(8):1627–1639, 1964.